



HAL
open science

zVAD-fmk upregulates caspase-9 cleavage and activity in etoposide-induced cell death of mouse embryonic fibroblasts

Aida Rodríguez-Enfedaque, Elisabeth Delmas, Arnaud Guillaume, Sébastien Gaumer, Bernard Mignotte, Jean-Luc Vayssière, Flore Renaud

► To cite this version:

Aida Rodríguez-Enfedaque, Elisabeth Delmas, Arnaud Guillaume, Sébastien Gaumer, Bernard Mignotte, et al.. zVAD-fmk upregulates caspase-9 cleavage and activity in etoposide-induced cell death of mouse embryonic fibroblasts. *Biochimica et Biophysica Acta - Molecular Cell Research*, 2012, 1823, pp.1343 - 1352. 10.1016/j.bbamcr.2012.05.013 . hal-02996979

HAL Id: hal-02996979

<https://hal.uvsq.fr/hal-02996979>

Submitted on 9 Nov 2020

HAL is a multi-disciplinary open access archive for the deposit and dissemination of scientific research documents, whether they are published or not. The documents may come from teaching and research institutions in France or abroad, or from public or private research centers.

L'archive ouverte pluridisciplinaire **HAL**, est destinée au dépôt et à la diffusion de documents scientifiques de niveau recherche, publiés ou non, émanant des établissements d'enseignement et de recherche français ou étrangers, des laboratoires publics ou privés.

zVAD-fmk upregulates caspase-9 cleavage and activity in etoposide-induced cell death of mouse embryonic fibroblasts.

Aida Rodríguez-Enfedaque, Elisabeth Delmas, Arnaud Guillaume, Sébastien Gaumer, Bernard Mignotte, Jean-Luc Vayssière and Flore Renaud.

Laboratoire de Génétique et Biologie Cellulaire, EA4589, Université de Versailles-Saint-Quentin-en-Yvelines, Ecole Pratique des Hautes Etudes, 45 avenue des Etats-Unis, 78035 Versailles Cedex, France.

Running title: Caspase-9 induces a mitochondrial amplification loop.

Corresponding author: Flore Renaud, Laboratoire de Génétique et Biologie Cellulaire, EA4589 UVSQ/EPHE, 45 avenue des Etats-Unis, 78035 Versailles, France. Tel: +33 1 39253658; Fax: +33 1 39253655; E-Mail: flore.renaud@uvsq.fr

ABSTRACT

Caspases are key effectors of programmed cell death. Down- and up-regulation of their activity are involved in different pathologies. In most cells, zVAD-fmk prevents apoptosis. However, unexpected effects of zVAD-fmk have been characterized in different laboratories, cell models and cell death processes. We have previously shown that zVAD-fmk accelerates p53-dependent apoptosis in rat embryonic fibroblasts. In this study, we pursued our investigations on zVAD-fmk effects and focused our study at the mitochondrial level in mouse embryonic fibroblasts (MEFs). In both primary and immortalized (by AgT or 3T9 protocol) MEFs, zVAD-fmk increased etoposide-induced loss of $\Delta\Psi_m$. This increase correlated with an increase of the number of apoptotic cells in primary and 3T9 MEFs, but did not in AgT MEFs. In both types of immortalized MEFs, zVAD-fmk regulated neither p53 levels nor transcriptional activities, suggesting that zVAD-fmk acts downstream of p53. In MEFs, zVAD-fmk increased p53-dependent loss of $\Delta\Psi_m$, cytochrome c release and caspase-9 activity. Indeed, zVAD-fmk inhibited effector caspases (caspases-3, -6, -7) as expected but increased caspase-9 cleavage and activity in etoposide-treated MEFs. Q-VD-OPh, another caspase inhibitor, also increased both loss of $\Delta\Psi_m$ and caspase-9 cleavage in etoposide-treated MEFs. Invalidation of *bax* and *bak* suppressed p53-dependent cell death and zVAD-fmk regulation of this process. Invalidation of *caspase-9* did not inhibit mitochondrial membrane depolarization but suppressed zVAD-fmk amplification of this process. Altogether, our data suggest that caspase-9 activity is up-regulated by zVAD-fmk and is involved in an amplification loop of etoposide-induced cell death at the mitochondrial level in MEFs.

Keywords : Caspase-9, zVAD-fmk, p53-dependent cell death, mouse embryonic fibroblasts

1. INTRODUCTION

Programmed cell death (PCD) is a physiological process required for embryogenesis, metamorphosis, tissue homeostasis and elimination of cells that are potentially detrimental to the organism. Misregulation of PCD has been implicated in many pathologies, such as cancers, neurodegenerative and autoimmune diseases [1, 2]. Different types of PCD have been described including apoptosis, necrosis and autophagy, which diverge on criteria such as the initiating death signals, morphological alterations, mitochondrial events, protease and/or nuclease activations, as well as functional and immunological aspects [3, 4]. We focused our study on mitochondrial-dependent cell death induced by the tumor suppressor p53. In response to stresses such as DNA damages, oncogene activation or hypoxia, the transcription factor p53 induces the intrinsic pathway of apoptosis [5, 6] by trans-activating genes encoding proteins involved in the induction of apoptosis, such as proapoptotic Bcl-2 family members (Bax, Puma or Noxa) [7, 8]. These proteins as well as p53 itself [9] can induce mitochondrial modifications, such as mitochondrial internal membrane depolarization and outer membrane permeabilization. These modifications induce the release of apoptogenic proteins, including cytochrome c and Smac/DIABLO, from the mitochondrial inter-membrane space to the cytosol. Cytochrome c release results in the formation of the apoptosome, a large complex composed of cytochrome c, ATP/dATP, Apaf-1 and procaspase-9. The formation of this apoptosome requires the interaction of Apaf-1 and procaspase-9 *via* their respective CARD domain, and activates the initiator caspase-9, which in turn activates effector caspases (caspase-3, -6 and -7) [10, 11]. Smac/DIABLO cooperates to the regulation of the apoptotic process by neutralizing the caspase-3, -7, -9 inhibitor XIAP in the cytosol [12, 13]. In some cell types, p53 also regulates the extrinsic apoptotic pathway by controlling the expression of genes coding for death receptor family members. This pathway is activated by death receptors able to cross-activate the intrinsic pathway *via* the caspase-8-dependent cleavage of Bid, a proapoptotic Bcl-2 family member [14].

A molecular hallmark of apoptosis is the activation of caspases, cysteinyl proteases that execute cell death through the cleavage of a broad spectrum of cellular protein targets after an Asp residue [11, 15-17]. Apoptotic caspases can be classified as initiator (caspase-2, -8, -9, -10) or effector caspases (caspase-3, -6, -7). The classical apoptotic pathways require a sequential activation of

initiator caspases (requiring adapter proteins) and effector caspases (cleaved by activated initiator or effector caspases). Most of the studies on both the function and the regulation of caspases have been performed using pharmacological inhibitors [18]. Benzyloxycarbonyl-Val-Ala-Asp(OMe)-fluoromethylketone (zVAD-fmk) is the most used cell permeable broad-caspase inhibitor. In most of the cells, zVAD-fmk prevents the apoptotic process. However, we have previously shown that zVAD-fmk increases p53-dependent cell death in rat embryonic fibroblasts [19-21]. In REtsAFs, a rat embryonic fibroblast cell line immortalized with a temperature-sensitive mutant (tsA58) of the simian virus 40 large tumor antigen (AgT), we have shown that p53-dependent cell death in the presence of zVAD-fmk diverges from the classical pathway. This cell death process induced in presence of zVAD-fmk could not be inhibited by Bcl-2 overexpression, in contrast to the classical pathway [19, 21]. Furthermore, we have shown that zVAD-fmk could modify p53-transcriptional activities in these cells. Indeed, p53-dependent trans-activation was decreased while p53-dependent trans-repression was increased in the presence of zVAD-fmk as shown by the study of p53 target genes expression and microarray analysis [20]. Different laboratories presented evidences that zVAD-fmk can induce switches between apoptotic, necrotic and autophagic cell deaths [22, 23] and that zVAD-fmk can not prevent all types of caspase-dependent apoptosis [19-21, 24, 25]. These unexpected effects of zVAD-fmk were detected on different cell death pathways, in different cell types and after different cell death stimuli. Altogether, these results suggest that the inability of zVAD-fmk to prevent some apoptotic cell deaths or to induce a switch in the cell death process might be due to the fact that this inhibitor does not inhibit all caspases to the same extent. To test this hypothesis and to progress in the comprehension of zVAD-fmk effect on p53-dependent cell death, we pursued our investigations on the zVAD-fmk effect in mouse embryonic fibroblasts (MEFs), in primary cultures and in immortalized cell lines issued from wild type, Bax^{-/-} Bak^{-/-} and caspase-9^{-/-} mice. In the present study, we show that: (i) zVAD-fmk accelerates mitochondrial membrane depolarization and cytochrome c release occurring during etoposide-induced cell death; (ii) although zVAD-fmk classically inhibited effector caspases, it did not inhibit the initiator caspase-9 but in contrast it induced the accumulation of the active form of this caspase; (iii) caspase-9 induces a mitochondrial amplification loop during etoposide-induced cell death in MEFs.

2. MATERIALS AND METHODS

2.1. Cell culture and drugs - Primary cultures of mouse embryonic fibroblasts (primary MEFs) were a generous gift from Alice Jouneau (INRA, Jouy-en-Josas, France). Established cell lines from wild type (3T9 MEFs) and *Bax^{-/-}Bak^{-/-}* (DKO 3T9 MEFs) mouse embryonic fibroblasts were a generous gift from Peter Daniel (Clinical and Molecular Oncology, University Medical Center Charité, Berlin, Germany). SV40 Antigen T immortalized MEFs from wild type (AgT MEFs) and Caspase-9^{-/-} (C9KO AgT MEFs) mice were a generous gift from Richard Flavell (Yale School of Medicine, Department of Immunology, New Haven, USA). MEFs were cultured in Dulbecco's modified Eagle's medium (DMEM, Invitrogen) supplemented with 10% (3T9, AgT, C9KO AgT and primary MEFs, HeLa cells) or 15% (DKO 3T9 MEFs) fetal bovine serum (FBS), 100 U/ml penicillin, 100 µg/ml streptomycin and 1% Glutamax at 37°C in 5% CO₂ humidified atmosphere. Etoposide (50 µg/ml, Sigma), which is an inhibitor of Topoisomerase II and a DNA damage-inducing drug, was used to induce p53-dependent cell death. zVAD-fmk (50 µM, Z-Val-Ala-DL-Asp-fluoromethylketone, Bachem) and Q-VD-OPh (20 µM, Quinolyl-Val-Asp-OPh, Biovision) were used as caspase inhibitors.

2.2. Flow cytometry analysis of cell death - Cells were plated in 12-well plates at a density of 7.10⁴ cells/ml. At 70% confluence, different treatments (etoposide, zVAD-fmk and/or Q-VD-OPh) were performed. Both attached and floating cells were collected and analyzed by flow cytometry after DiOC₆(3) and propidium iodide (PI) staining as previously described [26]. Three parameters were examined: the DiOC₆(3) staining (representative of the mitochondrial membrane potential, $\Delta\Psi_m$), cell size (representative of the condensation of the cells), and the PI staining (representative of primary or secondary necrotic cells). In this study, we focused our attention on: cells with low $\Delta\Psi_m$ which correspond to cells with low DiOC₆(3) and low PI staining cells; and, apoptotic cells which correspond to cells with small cell size, low DiOC₆(3) and low PI staining cells. MitoTracker® Red CMXRos was used to analyze the mitochondrial membrane potential of transfected cells. Cells were incubated with 150 nM MitoTracker® Red CMXRos for 30 min at 37°C before flow cytometry analysis.

2.3. ROS production analysis by flow cytometry - 3T9 MEFs cells and HeLa cells were plated in 12-well plates at a density of 7.10^4 cells/ml. At 70% confluence, etoposide and/or zVAD-fmk treatments were performed and reactive oxygen species (ROS) production was evaluated by flow cytometry after DCFH-DA staining as previously described (Dumay et al. 2006).

2.4. RT-PCR assay - At 70% confluence, 3T9 MEFs were incubated with or without etoposide +/- zVAD-fmk. After 16h of treatment, total RNA was isolated using the guanidium isothiocyanate method. RT-PCR was performed to examine the levels of p53, mdm2, p21 and noxa mRNAs as previously described [26]. RT-PCR of 18S rRNA was used as a control.

2.5. Cytosol fraction preparation - At 70% confluence, 3T9 MEFs were incubated with etoposide +/- zVAD-fmk for different treatment times (0, 4, 8, 12, 16 and 19 hours). Attached and floating cells were collected and centrifuged 5 min at 200 g. Pellets were resuspended in 200 μ L of Lysis buffer (10 mM HEPES-KOH pH 7.4, 0.1 mM EDTA, 1 mM EGTA, 250 mM Sucrose, 1 mM protease inhibitor cocktail AEBSF (Roche)). After 30 min incubation at 4°C, cell disruption was completed by passing the cells through a 0.4 x 20 mm needle 10 times. 1/3 of the extract was conserved as the total extract, 2/3 of the extract were centrifuged 5 min at 4°C at 52 g to eliminate nuclei. The supernatant was further centrifuged 30 min at 4°C at 7000 g to eliminate mitochondria and reticulum. The supernatant corresponded to the cytosol fraction and was analyzed by western blot.

2.6. Western blot analysis - At 70% confluence, MEFs were incubated with or without etoposide, zVAD-fmk and/or Q-VD-OPh. After different treatment times, cells were harvested, lysed and frozen at -20°C. Proteins (10-30 μ g), from total cell extracts or from cytosolic extracts, were separated in NuPAGE 4-12% Bis-Tris polyacrylamide gels according to the manufacturer's instructions (Invitrogen) and transferred onto a PVDF membrane (Millipore). The primary antibodies used were anti-p53 (Pab 122, gift from E. May, IRSC, Villejuif, France), anti-phospho-p53 (Ser-15, Cell Signaling), anti-actin (Sigma), anti-cytochrome c (BD Pharmingen), anti-VDAC (gift from C. Brenner, UVSQ, Versailles, France), anti-lamin A/C (Cell Signaling), anti-enolase (gift from N. Lamande, College de France, Paris), anti-caspase-9 (5B4, Abcam), anti-cleaved caspase-3 (Asp175, Cell Signaling), anti-cleaved caspase-6 (Asp162, Cell Signaling), and anti-tubulin (MAS078, Sera-Lab). Secondary antibodies (peroxidase-conjugated) were anti-rabbit, anti-mouse or anti-rat

immunoglobulin (Biosystem). Immunoreactive bands were detected by chemiluminescence using the Immobilon kit (Millipore).

2.7. Immunocytochemistry - 3T9 MEFs were plated onto glass coverslips in complete medium. At 60% confluence, cells were incubated with or without etoposide and/or zVAD-fmk. Immunocytochemistry analysis was performed as previously described [26]. In the present study, we used a mouse monoclonal anti-cytochrome c (BD Bioscience) as primary antibody and a FITC-conjugated anti-mouse antibody (Jackson ImmunoResearch Laboratory) as secondary antibody. Nuclei were stained with Hoechst 33342. Immunolabeled cells were examined by epifluorescence under a DMR Leica microscope equipped with an Olympus DP70 photo camera using the DP Manager software.

2.8. Caspase-3/7 and caspase-9 activity assays - The Apo-ONE™ Homogeneous Caspase-3/7 Assay and the Caspase-Glo™ 9 Assay (Promega) were used to detect caspase-3/-7 and caspase-9 activities in 3T9 MEFs treated with etoposide +/- zVAD-fmk according to the manufacturer's instructions.

2.9. Cell transfection – Caspase-9 KO AgT MEFs were plated in 12-well plates for flow cytometry analysis, and in 60 mm diameter plates for western-blot analysis at a density of 10^5 cells/ml. At 80% confluence, cells were transfected with 125 ng (for 12-well plate) or 1 µg (for 60 mm plate) pCDNA3-Caspase-9 expression vector in presence of Lipofectamine™ Transfection Reagent and PLUS™ Reagent in DMEM (Invitrogen) and incubated for 5 hours at 37°C according to the manufacturer's instructions. Human caspase-9 expression vector was a generous gift from Patrick Melhen (Apoptosis, Cancer and Development Laboratory, Centre Léon Bérard, Lyon, France). After 24 hours of culture in complete medium, transfected cells were incubated with etoposide for 16 hours. Then, the mitochondrial membrane potential was analyzed by flow cytometry after Mito Tracker Red CMXRos staining and cell lysates were analyzed by western-blot as previously described.

2.10. Statistical analysis – Each bar of the different graphs indicates the average measure and standard error of at least three independent experiments, and *P*-values are from paired two-tailed Student's *t*-tests.

3. RESULTS

3.1. zVAD-fmk increases etoposide-induced mitochondrial membrane depolarization in MEFs

In order to test the effect of zVAD-fmk on p53-dependent apoptosis in mouse embryonic fibroblasts (MEFs) that are either spontaneously immortalized (3T9 MEFs [27]), immortalized by transfection of SV40 AgT (AgT MEFs) or not immortalized (primary MEFs), we used etoposide, a DNA damage-inducing drug, to activate p53. The cell death process induced by etoposide in presence or absence of zVAD-fmk was analyzed by flow cytometry after DiOC₆(3) and propidium iodide (PI) staining (Figure 1). Apoptotic cells corresponded to the cells with three characteristics: low PI staining to exclude primary and secondary necrotic cells, low DiOC₆(3) staining indicating a low mitochondrial membrane potential $\Delta\Psi_m$, and low cell size (*i.e.* condensating cells). In AgT MEFs, etoposide increased the percentage of apoptotic cells and the addition of zVAD-fmk classically decreased this effect (Figure 1A). In 3T9 MEFs and in primary MEFs, zVAD-fmk surprisingly increased the percentage of apoptotic cells (Figure 1B, 1C). The effect of zVAD-fmk was more pronounced (earlier and higher) in primary MEFs than in the established cell line 3T9 MEFs, suggesting a physiological relevance of this process. Then, we analyzed the percentage of cells with low $\Delta\Psi_m$ (whatever the cell size) in the three types of MEFs. zVAD-fmk increased the percentage of cells with low $\Delta\Psi_m$ in primary and immortalized MEFs. Thus, these results suggest that: (i) zVAD-fmk differently affected late events of apoptosis, in particular cell condensation, depending on the immortalized state, (ii) zVAD-fmk accelerates the decrease of mitochondrial membrane potential in the three types of MEFs by acting either upstream or at the level of mitochondrial events.

zVAD-fmk has been reported to switch between different cell death modes (apoptosis, necrosis, autophagy, ...)[22, 23, 28]. In etoposide-treated MEFs, zVAD-fmk did not significantly increase necrosis, autophagy and LEI/L-DNaseII caspase-independent cell death (data not shown). Only apoptosis was detected to be regulated by zVAD-fmk in this cellular model.

3.2. zVAD-fmk does not modify p53 transcriptional activity after etoposide treatment in 3T9 MEFs

We have previously shown that zVAD-fmk modifies both p53 stability and p53-transcriptional activities in rat embryonic fibroblasts [20, 21]. Therefore, we examined the status of p53 (mRNA and

protein levels) and some of its targets (at the mRNA level) in the presence or absence of etoposide and/or zVAD-fmk in mouse embryonic fibroblasts. In 3T9 MEFs, addition of etoposide and/or zVAD-fmk did not modify the levels of p53 mRNAs and protein (Figure 2). In contrast, addition of etoposide induced an increase of the level in serine 15-phosphorylated p53 (Figure 2B) as well as in mdm2, p21 and noxa mRNA levels (Figure 2A), showing that etoposide induces p53-transcriptional activity. The addition of zVAD-fmk modified neither the p53 levels nor the mRNA levels of p53 targets in the presence of etoposide, suggesting that zVAD-fmk does not regulate p53-transcriptional activity in 3T9 MEFs. Altogether, these results suggest that zVAD-fmk increases mitochondrial membrane depolarization downstream of p53 transcriptional activity in mouse embryonic fibroblasts after etoposide treatment.

3.3. Bax and/or Bak are involved in etoposide-induced cell death in the presence or absence of zVAD-fmk

We then examined the possible involvement of Bax/Bak or reactive oxygen species (ROS) accumulation in the cell death process occurring in 3T9 MEFs after etoposide treatment in absence or in presence of zVAD-fmk.

To determine whether Bax and Bak are required for etoposide-induced cell death and for the regulation of this process by zVAD-fmk, we used DKO 3T9 MEFs (Bax^{-/-}Bak^{-/-} double knockout MEFs [29]). Mitochondrial membrane depolarization, as assessed by flow cytometric $\Delta\Psi_m$ analysis, induced by etoposide in the presence or absence of zVAD-fmk in 3T9 MEFs (after 16 hours of treatment) was not detected in DKO 3T9 MEFs even after longer treatments (16 and 45 hours of treatment) (Figure 3A). Our results show that Bax and/or Bak are required for etoposide-induced loss of $\Delta\Psi_m$ and for zVAD-fmk-induced increase of this depolarization in mouse embryonic fibroblasts.

ROS accumulation could be involved in mitochondrial-membrane potential collapse and cell death. Thus, we examined ROS production induced by etoposide in 3T9 MEF cells in the absence or presence of zVAD-fmk by flow cytometry after DCFH-DA staining. Whatever the treatment (etoposide +/- zVAD-fmk), DCF positive 3T9 MEFs could not be detected by flow cytometry in contrast to DCF positive etoposide-treated HeLa cells, which were used as positive control (Figure

3B). This result suggests that etoposide in the presence or absence of zVAD-fmk does not activate ROS production in mouse embryonic fibroblasts.

3.4. zVAD-fmk increases cytochrome c release after etoposide-treatment

We then examined the release of cytochrome c from mitochondria to the cytosol after etoposide-treatment in the presence or absence of zVAD-fmk in 3T9 MEFs. Immunocytochemistry experiments show that cytochrome c was principally detected in the mitochondria in the absence of cell death inducer (Figure 4A, 4B). After etoposide treatment, cytochrome c release to the cytosol was detected in about 10 % of the cells. The addition of zVAD-fmk increased the percentage of cells with cytochrome c release in presence of etoposide up to 34 %. zVAD-fmk alone had no effect on cytochrome c localization. After etoposide treatment in the presence or absence of zVAD-fmk, dying cells detached from the Petri dish. Thus, we analyzed the level of cytosolic cytochrome c in all cells (both attached and floating cells) after cytosolic extraction and western-blot analysis (Figure 4C). The detection of cytosolic enolase and the absence of detection of both mitochondrial VDAC and nuclear lamin A/C in the cytosolic fractions confirmed the efficiency of the enrichment. All these proteins could be detected in total cell extracts (control lanes). The amount of cytochrome c detected in the cytosolic fractions after etoposide treatment strongly increased in the presence of zVAD-fmk. Thus, we have shown that zVAD-fmk increases cytochrome c release after etoposide treatments in mouse embryonic fibroblasts by two experimental processes.

3.5. zVAD-fmk upregulates initiator caspase-9 but downregulates effector caspases after etoposide treatment

In most of the cells, cytochrome c release induced the formation of the apoptosome and the activation of initiator caspase-9 and effector caspases (-3, -6 and -7). We studied the cleavage and activity status of these caspases in 3T9 MEFs treated with etoposide and/or zVAD-fmk. After etoposide treatment, cleaved forms of caspase-9, caspase-3 and caspase-6 were detected in 3T9 MEFs by western-blot (Figure 5A). Surprisingly, the addition of zVAD-fmk in the presence of etoposide increased the level of cleaved caspase-9, while zVAD-fmk modified caspase-3 cleavage and inhibited

caspase-6 cleavage. An upper cleaved form of caspase-3 was detected in the presence of zVAD-fmk, which probably corresponded to an incompletely cleaved form of this caspase.

To determine whether the cleaved forms of caspase-9 and caspases-3 detected in the presence of etoposide and zVAD-fmk were functional, we measured caspase-9 and caspase-3/-7 activities. In 3T9 MEFs, the etoposide treatment increased both caspase-9 (Figure 5B) and caspase-3/-7 (Figure 5C) activities. Adding zVAD-fmk down-regulated caspase-3/-7 activity but, in contrast, up-regulated caspase-9 activity in mouse embryonic fibroblasts.

In most cells, caspase-6 is cleaved by active caspase-3. The absence of caspase-6 cleavage in the presence of etoposide and zVAD-fmk in 3T9 MEFs (Figure 5A) suggested that caspase-6 is cleaved by caspase-3 in etoposide-treated MEF cells and that zVAD-fmk inhibited caspase-6 by inhibiting caspase-3. Etoposide treatment in the absence of zVAD-fmk induced lamin A/C cleavage (a caspase-6 substrate) in 3T9 MEFs suggesting caspase-6 activation in this condition. Addition of zVAD-fmk inhibited both etoposide-induced caspase-6 activity and lamin A/C cleavage in 3T9 MEFs cells.

Altogether, our data showed that during etoposide-induced apoptosis, zVAD-fmk classically inhibited effector caspases in mouse embryonic fibroblasts but surprisingly, increased caspase-9 activity.

3.6. Q-VD-OPh increased etoposide-induced loss of $\Delta\Psi_m$ and caspase-9 cleavage in 3T9 MEFs

We tested another broad-spectrum caspase inhibitor, Q-VD-OPh in 3T9 MEFs. As zVAD-fmk, Q-VD-OPh increased etoposide-induced loss of mitochondrial membrane potential as assessed by flow cytometry analysis of $\Delta\Psi_m$ (Figure 1B, 3A, 6A). We also showed by western-blot (Figure 6B) that Q-VD-OPh increased the level of etoposide-induced cleaved caspase-9 and modified caspase-3 cleavage, to the same extent as zVAD-fmk. Thus, using two different caspase inhibitors, zVAD-fmk and Q-VD-OPh, we demonstrated a correlation between the loss of $\Delta\Psi_m$ and caspase-9 cleavage in 3T9 MEFs.

3.7. Caspase-9 activates an amplification loop at the mitochondrial level

Our study suggests that caspase-9 is a key caspase in the mitochondrial membrane depolarization induced by etoposide in the presence of zVAD-fmk in 3T9 MEFs. In an attempt to progress in the characterization of its function, we analyzed the process induced by etoposide in the presence or in the absence of zVAD-fmk in a mouse embryonic fibroblast cell line issued from *caspase-9* knock-out mice (*caspase-9^{-/-}* AgT MEFs).

First, we controlled that etoposide induces p53 transcriptional activity in *caspase-9^{-/-}* AgT MEFs to the same extent as in control AgT MEFs issued from wild type mice (Figure 7A). Analysis by RT-PCR showed that etoposide in the presence or absence of zVAD-fmk induced a similar increase of noxa, mdm2 and p21 mRNA levels in both cell lines.

Then, we examined the status of caspase-9 and caspase-3 in these cell lines (Figure 7B). In *caspase-9^{-/-}* AgT MEFs, no proform or cleaved caspase-9 was detected whatever the treatment in contrast to control AgT MEFs. In these control cells, zVAD-fmk increased the level of cleaved caspase-9 after etoposide treatment as previously shown in 3T9 MEFs. In *caspase-9^{-/-}* AgT MEFs, we did not detect cleaved caspase-3 whatever the treatment, showing that caspase-9 is required for caspase-3 activation in MEFs cells after etoposide treatment.

We further analyzed mitochondrial membrane depolarization by cytometry after DiOC₆(3) and PI staining (Figure 7C). Etoposide treatment increased the percentage of cells loosing $\Delta\Psi_m$ at a similar level in both cell lines. The addition of zVAD-fmk in the presence of etoposide increased this effect in AgT MEFs. In *caspase-9^{-/-}* AgT MEFs, the percentage of cells with a loss of $\Delta\Psi_m$ after etoposide treatment was not modified by the presence of zVAD-fmk. Thus, although caspase-9 is not required for etoposide-dependent mitochondrial membrane depolarization, caspase-9 activity is required for the amplification of this process by zVAD-fmk.

To confirm that caspase-9 can induce an increase of mitochondrial membrane depolarization, we expressed caspase-9 in *caspase-9^{-/-}* AgT MEFs by transfection and analyzed the loss of $\Delta\Psi_m$ in absence or in presence of etoposide in transfected cells (Figure 7D, 7E). In absence of etoposide, overexpression of caspase-9 (both proform and cleaved forms could be detected) induced loss of $\Delta\Psi_m$

to the same extent as etoposidetreated control cells. In presence of etoposide, cleaved caspase-9 level increased as well as loss of $\Delta\Psi_m$ induced in caspase-9 transfected cells. Thus, overexpression of caspase-9 in caspase-9^{-/-} AgT MEFs increased mitochondrial membrane depolarization induced by etoposide. Altogether, our data show that caspase-9, which was up-regulated by zVAD-fmk or by transfection, induces an amplification loop at the mitochondrial level of the cell death process induced by etoposide in MEFs.

4. DISCUSSION

In the present study, we examined the effect of zVAD-fmk in etoposide-induced cell death in mouse embryonic fibroblasts and showed that zVAD-fmk can regulate this cell death process at the mitochondrial level. Indeed, zVAD-fmk increased etoposide-induced mitochondrial membrane depolarization in MEFs, whether the cells were immortalized (3T9 and AgT MEFs) or not (Figure 1 and 7). The effect of zVAD-fmk on $\Delta\Psi_m$ was correlated with an increase in the number of apoptotic cells in primary and 3T9 MEFs. This correlation was not detected in AgT MEFs. However, longer etoposide treatment in the presence of zVAD-fmk induced late events of apoptosis, like cell size reduction and DNA fragmentation (data not shown). Our results suggest that immortalization of MEFs by the AgT could modify the level and/or the activity of factors involved in late events of the apoptotic process (nuclear and/or cell condensation) compared to primary MEFs. These modifications remain to be characterized.

In both immortalized MEFs (AgT and 3T9 MEFs), zVAD-fmk modified neither p53 mRNA and protein levels nor p53 transcriptional activities (in particular the trans-activation of *noxa*, *mdm2* and *p21*) induced in the presence of etoposide (Figures 2, 7). The regulations of p53-transcriptional activities induced by zVAD-fmk characterized in rat embryonic fibroblasts [20] were not detected in MEFs. These differences between both cellular models could reflect either differences in cellular contents between rat and mouse, or differences in the p53 induction mode (etoposide treatment in MEFs *versus* temperature increase in REtsAF cell lines). Our unpublished data are in favor of the first hypothesis. In etoposide-treated REtsAF cells, zVAD-fmk increased p53 stability and phosphorylation (Ser-15) as well as *puma* trans-activation (data not shown). These data suggest that the effect of

zVAD-fmk on etoposide-induced cell death is located downstream of p53 regulation in MEFs. We thus focused our study on mitochondrial events and showed that zVAD-fmk accelerates the loss of $\Delta\Psi_m$, cytochrome c release in the cytosol and caspase-9 activation in etoposide-treated 3T9 MEFs (Figures 1, 4, 5). We also showed that Bax and Bak are required for etoposide-induced loss of $\Delta\Psi_m$ in the absence or presence of zVAD-fmk, in contrast to ROS production that was not detected in MEF cells (Figure 3). These data let us hypothesize that zVAD-fmk could induce an amplification loop of an etoposide-induced cell death at the mitochondrial level in MEFs.

Two presumed broad caspase inhibitors, zVAD-fmk and Q-VD-Oph, increased etoposide-induced loss of $\Delta\Psi_m$ in 3T9 MEFs (Figures 1, 6), suggesting that both drugs act *via* the regulation of caspase activities. The study of caspase activities by analysis of their cleavage, activity and/or the cleavage of specific targets after etoposide treatment in MEFs (Figure 5, 6, 7) showed that: (i) zVAD-fmk classically inhibited effector caspases (*i.e.* caspase-3, -6 and -7), (ii) zVAD-fmk did not inhibit the initiator caspase-9 and in contrast induced an increase of the active forms of this caspase, (iii) Q-VD-Oph induced an accumulation of auto-cleaved caspase-9. One hypothesis to explain these data is that the catalytic site of the proform and the auto-cleaved form of caspase-9 could not be accessible to zVAD-fmk, and to Q-VD-Oph, due to their integration into the apoptosome and/or post-translational modifications (such as phosphorylation). Indeed, the activation of caspase-9 and its regulations are quite complex [11, 16, 30-34]. Caspase-9 is activated through autocatalytic intra-chain cleavages into the apoptosome, and at least two cleavages are involved in the generation of mature caspase-9. The pro-, auto-cleaved and mature forms present caspase activity. However, conformational and catalytic specificities of these forms differ. Two previous reports have shown that zVAD-fmk does not inhibit the auto-cleavage of procaspase-9 while it inhibits procaspase-3 cleavage by mature caspase-9 [32, 35], suggesting that zVAD-fmk inhibits only mature forms of caspase-9. In the presence of etoposide, zVAD-fmk inhibited neither the auto-cleavage of procaspase-9 nor the processing of procaspase-3 by caspase-9, suggesting that zVAD-fmk does not inhibit any of the different forms of caspase-9 in MEFs. zVAD-fmk inhibited the last processing step of caspase-3 cleavage, which requires caspase-3 activity and not caspase-9 activity. The increase in both auto-cleaved caspase-9 level and caspase-9

activity could be the result of an increase in the auto-cleavage process and/or the result of an inhibition of the degradation of cleaved caspase-9. zVAD-fmk increases mitochondrial membrane depolarization and cytochrome c release suggesting that it can result in an increase at the cell level in apoptosome activity and thus in an increase of auto-cleaved caspase-9 levels in presence of zVAD-fmk. However, we cannot exclude the hypothesis that zVAD-fmk could also regulate the proteasome activity and that accumulation of auto-cleaved caspase-9 could result in part from this regulation. Interactions between cell death and proteasomal degradation were previously characterized [35, 36]. In collaboration with Isabelle Petropoulos (Université Pierre et Marie Curie, UR4 « Vieillissement, Stress et Inflammation », Paris), we studied proteasomal activities (in particular, chymotrypsin-like, post-glutamic hydrolase and trypsin-like activities) in 3T9 MEFs in the absence or in the presence of etoposide and zVAD-fmk. No significant modification of these activities was detected in the presence of etoposide +/- zVAD-fmk, in contrast to what was observed in TNF α -treated 3T9 MEFs (unpublished data) showing that accumulation of caspases-9 does not result from an unspecific proteasome inhibition.

Altogether, our results indicate that caspases-9 activates an amplification loop at the mitochondrial level during the cell death process induced by etoposide in mouse embryonic fibroblasts. To test this hypothesis, we used AgT MEFs issued from caspase-9^{-/-} mice (AgT MEFs KOC9, Figure 7). In these cells, etoposide induced mitochondrial membrane depolarization to the same extent in the presence or in the absence of zVAD-fmk, which shows that the absence of caspase-9 completely abolished the acceleration of the loss of $\Delta\Psi_m$ induced by zVAD in MEFs. In caspase-9^{-/-} AgT MEFs, reexpression of caspase-9 increased etoposide-induced mitochondrial membrane depolarization. The correlation between cleaved caspase-9 level and loss of $\Delta\Psi_m$ suggests that caspase-9 induces mitochondrial membrane depolarization and an amplification loop of the cell death process induced by etoposide. Thus, although caspase-9 is not required for etoposide-induced loss of $\Delta\Psi_m$ in MEFs cells, caspase-9 is required for the amplification of this process by zVAD-fmk. Such a positive feedback loop at the mitochondrial level could involve a cleavage of an anti-apoptotic member of the Bcl-2 family as described in other systems [37, 38].

In conclusion, we demonstrate here for the first time that caspase-9, which is up-regulated by zVAD-fmk, induces an amplification loop at the mitochondrial level of the cell death process induced by etoposide in mouse embryonic fibroblasts.

5. ACKNOWLEDGEMENTS

This work was supported in part by grants from the “Association pour la Recherche Contre le Cancer” (#3819) and the “Ligue Nationale Contre le Cancer”. Aida Rodriguez-Enfedaque and Elisabeth Delmas were supported by fellowships from the “Ministère de l’Education Nationale, de l’Enseignement Supérieur et de la Recherche”.

6. REFERENCES

- [1] C. Twomey and J.V. McCarthy, Pathways of apoptosis and importance in development, *J Cell Mol Med* 9 (2005) 345-59.
- [2] B. Fadeel and S. Orrenius, Apoptosis: a basic biological phenomenon with wide-ranging implications in human disease, *J Intern Med* 258 (2005) 479-517.
- [3] M. Bras, B. Queenan and S.A. Susin, Programmed cell death via mitochondria: different modes of dying, *Biochemistry (Mosc)* 70 (2005) 231-9.
- [4] G. Kroemer, L. Galluzzi, P. Vandenabeele, J. Abrams, E.S. Alnemri, E.H. Baehrecke, M.V. Blagosklonny, W.S. El-Deiry, P. Golstein, D.R. Green, M. Hengartner, R.A. Knight, S. Kumar, S.A. Lipton, W. Malorni, G. Nunez, M.E. Peter, J. Tschopp, J. Yuan, M. Piacentini, B. Zhivotovsky and G. Melino, Classification of cell death: recommendations of the Nomenclature Committee on Cell Death 2009, *Cell Death Differ* 16 (2009) 3-11.
- [5] M.F. Lavin and N. Gueven, The complexity of p53 stabilization and activation, *Cell Death Differ* 13 (2006) 941-50.
- [6] L. Bai and W.-G. Zhu, p53: Structure, Function and Therapeutic Applications, *Journal of Cancer Molecules* 2 (2006) 141-153.
- [7] J. Yu and L. Zhang, The transcriptional targets of p53 in apoptosis control, *Biochem Biophys Res Commun* 331 (2005) 851-8.
- [8] R.J. Youle and A. Strasser, The BCL-2 protein family: opposing activities that mediate cell death, *Nat Rev Mol Cell Biol* 9 (2008) 47-59.
- [9] U.M. Moll, S. Wolff, D. Speidel and W. Deppert, Transcription-independent pro-apoptotic functions of p53, *Curr Opin Cell Biol* 17 (2005) 631-6.
- [10] Y.P. Ow, D.R. Green, Z. Hao and T.W. Mak, Cytochrome c: functions beyond respiration, *Nat Rev Mol Cell Biol* 9 (2008) 532-42.
- [11] Q. Bao and Y. Shi, Apoptosome: a platform for the activation of initiator caspases, *Cell Death Differ* 14 (2007) 56-65.
- [12] A.M. Verhagen, E.J. Coulson and D.L. Vaux, Inhibitor of apoptosis proteins and their relatives: IAPs and other BIRPs, *Genome Biol* 2 (2001) REVIEWS3009.
- [13] P. Liston, W.G. Fong and R.G. Korneluk, The inhibitors of apoptosis: there is more to life than Bcl2, *Oncogene* 22 (2003) 8568-80.
- [14] H. Li, H. Zhu, C.J. Xu and J. Yuan, Cleavage of BID by caspase 8 mediates the mitochondrial damage in the Fas pathway of apoptosis, *Cell* 94 (1998) 491-501.
- [15] U. Fischer, R.U. Janicke and K. Schulze-Osthoff, Many cuts to ruin: a comprehensive update of caspase substrates, *Cell Death Differ* 10 (2003) 76-100.

- [16] P. Fuentes-Prior and G.S. Salvesen, The protein structures that shape caspase activity, specificity, activation and inhibition, *Biochem J* 384 (2004) 201-32.
- [17] S.J. Riedl and Y. Shi, Molecular mechanisms of caspase regulation during apoptosis, *Nat Rev Mol Cell Biol* 5 (2004) 897-907.
- [18] I.T. Weber, B. Fang and J. Agniswamy, Caspases: structure-guided design of drugs to control cell death, *Mini Rev Med Chem* 8 (2008) 1154-62.
- [19] V. Rincheval, F. Renaud, C. Lemaire, B. Mignotte and J.L. Vayssiere, Inhibition of Bcl-2-dependent cell survival by a caspase inhibitor: a possible new pathway for Bcl-2 to regulate cell death, *FEBS Lett* 460 (1999) 203-6.
- [20] N. Godefroy, S. Bouleau, G. Gruel, F. Renaud, V. Rincheval, B. Mignotte, D. Tronik-Le Roux and J.L. Vayssiere, Transcriptional repression by p53 promotes a Bcl-2-insensitive and mitochondria-independent pathway of apoptosis, *Nucleic Acids Res* 32 (2004) 4480-90.
- [21] N. Godefroy, C. Lemaire, F. Renaud, V. Rincheval, S. Perez, I. Parvu-Ferecatu, B. Mignotte and J.L. Vayssiere, p53 can promote mitochondria- and caspase-independent apoptosis, *Cell Death Differ* 11 (2004) 785-7.
- [22] P. Vandenabeele, T. Vanden Berghe and N. Festjens, Caspase inhibitors promote alternative cell death pathways, *Sci STKE* 2006 (2006) pe44.
- [23] C. Scheller, J. Knoferle, A. Ullrich, J. Pröttengeier, T. Racek, S. Sopper, C. Jassoy, A. Rethwilm and E. Koutsilieri, Caspase inhibition in apoptotic T cells triggers necrotic cell death depending on the cell type and the proapoptotic stimulus, *J Cell Biochem* 97 (2006) 1350-61.
- [24] S.O. Kim, K. Ono and J. Han, Apoptosis by pan-caspase inhibitors in lipopolysaccharide-activated macrophages, *Am J Physiol Lung Cell Mol Physiol* 281 (2001) L1095-105.
- [25] S.B. Yee, S.J. Baek, H.T. Park, S.H. Jeong, J.H. Jeong, T.H. Kim, J.M. Kim, B.K. Jeong, B.S. Park, T.K. Kwon, I. Yoon and Y.H. Yoo, zVAD-fmk, unlike BocD-fmk, does not inhibit caspase-6 acting on 14-3-3/Bad pathway in apoptosis of p815 mastocytoma cells, *Exp Mol Med* 38 (2006) 634-42.
- [26] S. Bouleau, I. Parvu-Ferecatu, A. Rodriguez-Enfedaque, V. Rincheval, H. Grimal, B. Mignotte, J.L. Vayssiere and F. Renaud, Fibroblast Growth Factor 1 inhibits p53-dependent apoptosis in PC12 cells, *Apoptosis* 12 (2007) 1377-87.
- [27] G.J. Todaro and H. Green, Quantitative studies of the growth of mouse embryo cells in culture and their development into established lines, *J Cell Biol* 17 (1963) 299-313.
- [28] A. Torriglia, C. Lepretre, L. Padron-Barthe, S. Chahory and E. Martin, Molecular mechanism of L-DNase II activation and function as a molecular switch in apoptosis, *Biochem Pharmacol* 76 (2008) 1490-502.
- [29] M.C. Wei, W.X. Zong, E.H. Cheng, T. Lindsten, V. Panoutsakopoulou, A.J. Ross, K.A. Roth, G.R. MacGregor, C.B. Thompson and S.J. Korsmeyer, Proapoptotic BAX and BAK: a requisite gateway to mitochondrial dysfunction and death, *Science* 292 (2001) 727-30.
- [30] S.M. Srinivasula, M. Ahmad, T. Fernandes-Alnemri and E.S. Alnemri, Autoactivation of procaspase-9 by Apaf-1-mediated oligomerization, *Mol Cell* 1 (1998) 949-57.
- [31] H.R. Stennicke, Q.L. Deveraux, E.W. Humke, J.C. Reed, V.M. Dixit and G.S. Salvesen, Caspase-9 can be activated without proteolytic processing, *J Biol Chem* 274 (1999) 8359-62.
- [32] P. Saikumar, M. Mikhailova and S.L. Pandeswara, Regulation of caspase-9 activity by differential binding to the apoptosome complex, *Front Biosci* 12 (2007) 3343-54.
- [33] L.A. Allan and P.R. Clarke, Apoptosis and autophagy: Regulation of caspase-9 by phosphorylation, *Febs J* 276 (2009) 6063-73.
- [34] S. Malladi, M. Challa-Malladi, H.O. Fearnhead and S.B. Bratton, The Apaf-1*procaspase-9 apoptosome complex functions as a proteolytic-based molecular timer, *Embo J* 28 (2009) 1916-25.
- [35] X.M. Sun, M. Butterworth, M. MacFarlane, W. Dubiel, A. Ciechanover and G.M. Cohen, Caspase activation inhibits proteasome function during apoptosis, *Mol Cell* 14 (2004) 81-93.
- [36] V. Jesenberger and S. Jentsch, Deadly encounter: ubiquitin meets apoptosis, *Nat Rev Mol Cell Biol* 3 (2002) 112-21.

- [37] M. Chen, A.D. Guerrero, L. Huang, Z. Shabier, M. Pan, T.H. Tan and J. Wang, Caspase-9-induced mitochondrial disruption through cleavage of anti-apoptotic BCL-2 family members, *J Biol Chem* 282 (2007) 33888-95.
- [38] P. Gomez-Bougie, L. Oliver, S. Le Gouill, R. Bataille and M. Amiot, Melphalan-induced apoptosis in multiple myeloma cells is associated with a cleavage of Mcl-1 and Bim and a decrease in the Mcl-1/Bim complex, *Oncogene* 24 (2005) 8076-9.

7. TITLES AND LEGENDS TO FIGURES

Figure 1: zVAD-fmk increases mitochondrial membrane depolarization in MEFs after etoposide treatment. AgT MEFs (A), 3T9 MEFs (B) and Primary MEFs (C) were untreated or treated with etoposide, both etoposide and zVAD-fmk or zVAD-fmk. After 16 hours (for AgT and 3T9 MEFs) or 12 hours (for primary MEFs) of treatment, all the cells (attached and floating) were analyzed by flow cytometry after DiOC₆(3) and PI staining. Apoptotic cells are characterized by a low PI staining to exclude primary and secondary necrotic cells, a low DiOC₆(3) staining that correlates with low mitochondrial membrane potential $\Delta\Psi_m$ and a low cell size that reveals cell condensation and late apoptotic events. Cells with low $\Delta\Psi_m$ display a low PI and low DiOC₆(3) staining whatever the size of the cells. Average and Student's t tests were performed to compare etoposide *versus* etoposide and zVAD-fmk (*p<0.05).

Figure 2: zVAD-fmk does not affect p53 levels or p53 transcriptional activity in 3T9 MEFs. (A) RT-PCR analysis of p53, mdm2, noxa and p21 mRNAs in 3T9 MEFs incubated with etoposide +/- zVAD-fmk during 16 hours. An 18S rRNA RT-PCR amplification is used as a control. (B) The levels of p53, p53P (Ser 15) and actin were detected by western blot in 3T9 MEFs cultured as in (A).

Figure 3: Bax, Bak and PTP involvement in etoposide-induced loss of $\Delta\Psi_m$ in 3T9 MEFs in the presence or absence of zVAD-fmk. (A) 3T9 MEFs and DKO 3T9 MEFs (Bax^{-/-}Bak^{-/-} double knockout MEFs) were incubated with etoposide +/- zVAD-fmk for 16 or 45 hours. Mitochondrial membrane depolarization was analyzed by flow cytometry after DiOC₆(3)/PI staining. (B) 3T9 MEFs and HeLa cells were incubated with etoposide +/- zVAD-fmk for 20 hours and ROS production was evaluated by cytometry after DCF-DA staining.

Figure 4: zVAD-fmk increases cytochrome c release after etoposide-treatment in 3T9 MEFs. (A) 3T9 MEFs were incubated with etoposide +/- zVAD-fmk for 16 hours. Immunostaining of cytochrome c (green) and nuclei labeling with Hoechst (blue) are presented. (B) The percentage of

cells with released cytochrome c was quantified from immunocytochemistry experiments; 200 to 300 cells were analyzed for each treatment. Student's t tests were performed (*p<0.01). (C) Cytosolic fractions were isolated from 3T9 MEFs treated with etoposide and/or zVAD-fmk for 0, 4, 8, 12, 16 or 19 hours. Total cell extracts (control) and cytosolic fractions were analyzed by western-blot to examine the levels of cytochrome c, VDAC, lamin A/C and enolase.

Figure 5: zVAD-fmk up-regulates caspase-9 and down-regulates effector caspases in 3T9 MEFs.

(A) 3T9 MEFs were treated with etoposide +/- zVAD-fmk for 18 hours. Caspase-9 (proform and cleaved form), cleaved caspase-3, cleaved caspase-6, lamin A/C (normal and cleaved forms) were detected by western-blot. Tubulin detection was used as a control. (B, C) After etoposide +/- zVAD-fmk treatment, caspase-9 (B) and caspase-3/-7 (C) activities in 3T9 MEFs were quantified using luminescence (RLU) or fluorescence (RFU) specific caspase activity assays. Student's t tests were performed (*p<0.05, **p<0.01).

Figure 6: Q-VD-Oph increases etoposide-induced loss of $\Delta\Psi_m$ and caspase-9 cleavage in 3T9 MEFs.

(A) 3T9 MEFs were untreated or treated with etoposide, etoposide and Q-VD-Oph or Q-VD-Oph for 16 hours. Cells with mitochondrial membrane depolarization were analyzed by flow cytometry after DiOC₆(3)/PI staining. Student's t tests were performed (*p<0.01). (B) 3T9 MEFs were treated with etoposide +/- Q-VD-Oph +/- zVAD-fmk. Caspase-9 (proform and cleaved form), cleaved caspase-3 and actin were analyzed by western-blot.

Figure 7: Caspase-9 induces an amplification loop at the mitochondrial level.

(A, B, C) AgT MEFs and Caspase-9^{-/-} AgT MEFs were incubated with etoposide +/- zVAD-fmk for 16 hours. noxa, mdm2, p21 mRNA and 18S rRNA levels were analyzed by RT-PCR (A). Caspase-9 (proform and cleaved form), cleaved caspase-3 and actin levels were analyzed by Western-blot (B). Cells with mitochondrial membrane depolarization were analyzed by flow cytometry after DiOC₆(3)/PI staining (C). Student's t tests were performed (*p<0.001, ns: no significant difference, n=7). (D, E) Caspase-9^{-/-} AgT MEFs were transfected by a human caspase-9 expression vector and incubated with etoposide for

16 hours. Cells with mitochondrial membrane depolarization were analysed by flow cytometry after CMX-ros staining (D). Caspase-9 (proform and cleaved form) and actin levels were analysed by Western-blot (E). Student's t tests were performed (* $p < 0.001$, ns: no significant difference, $n=3$).

Figure 1

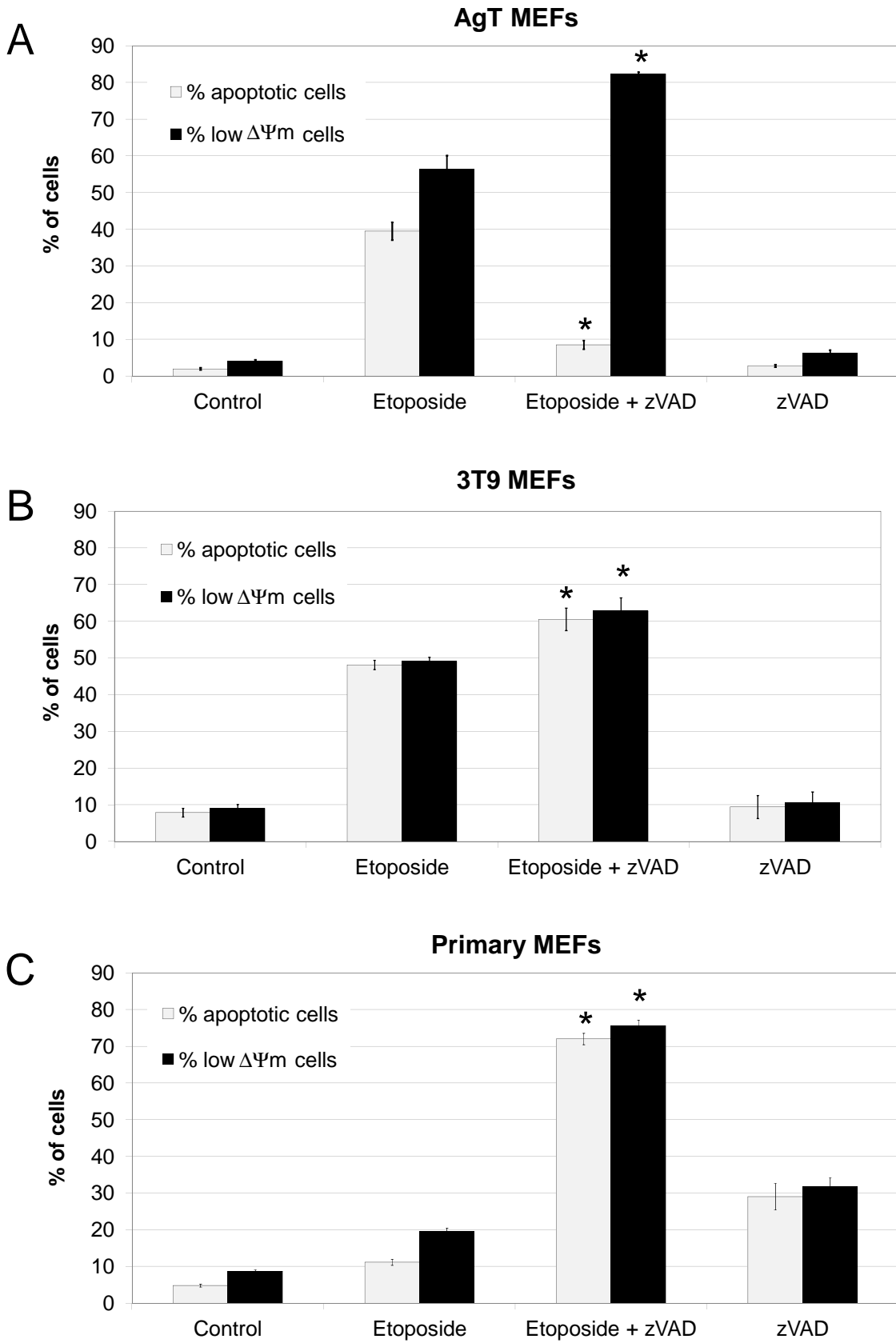
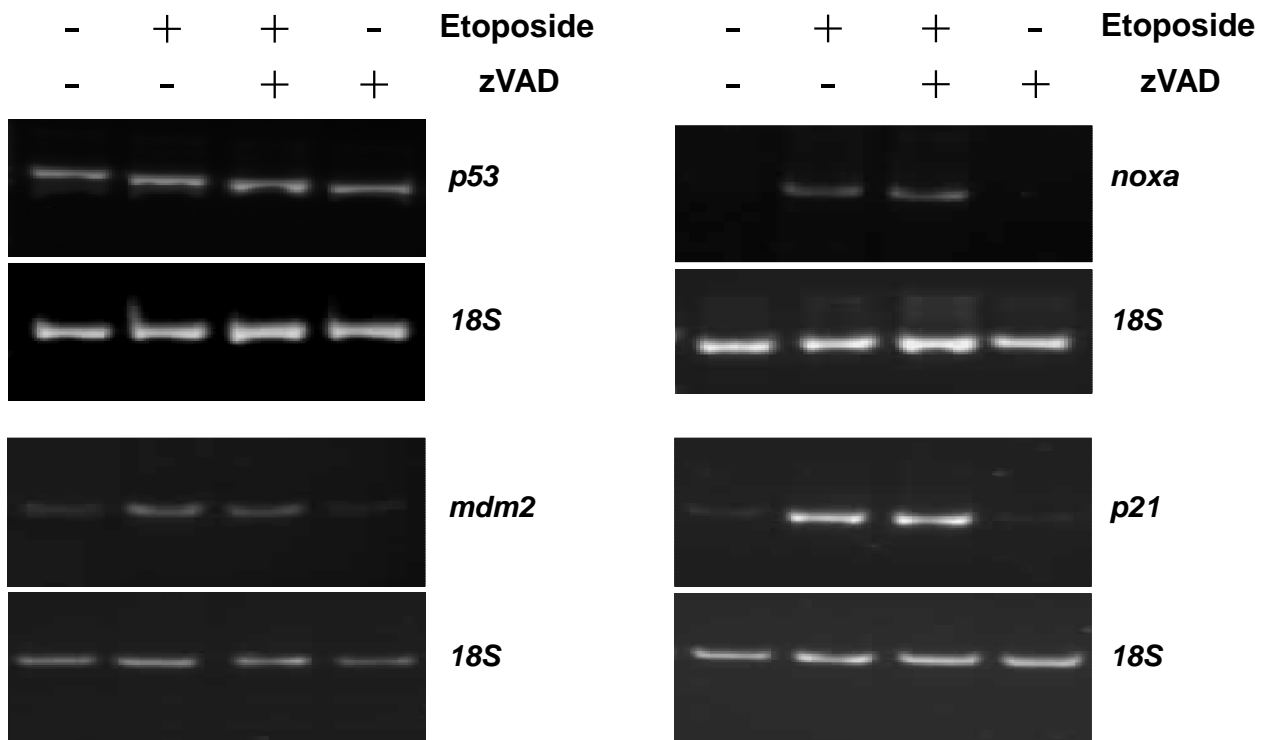


Figure 2

A



B

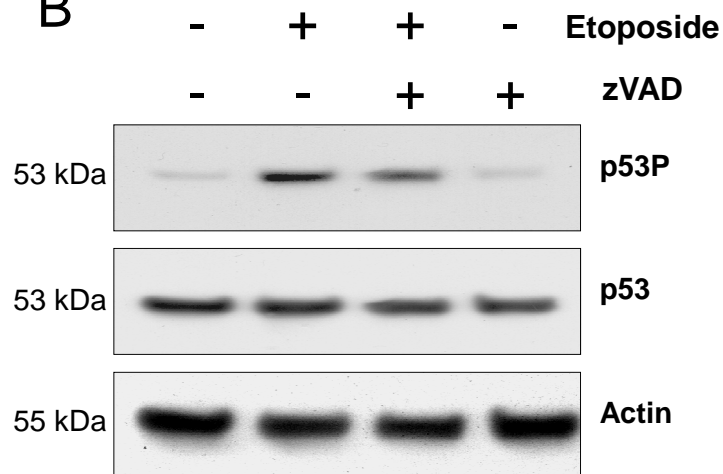


Figure 3

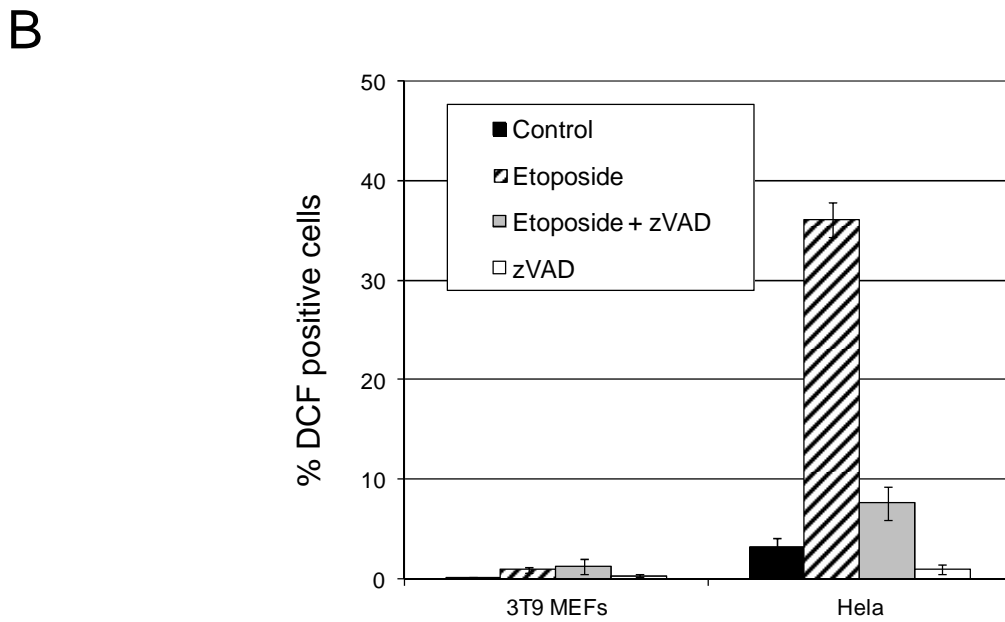
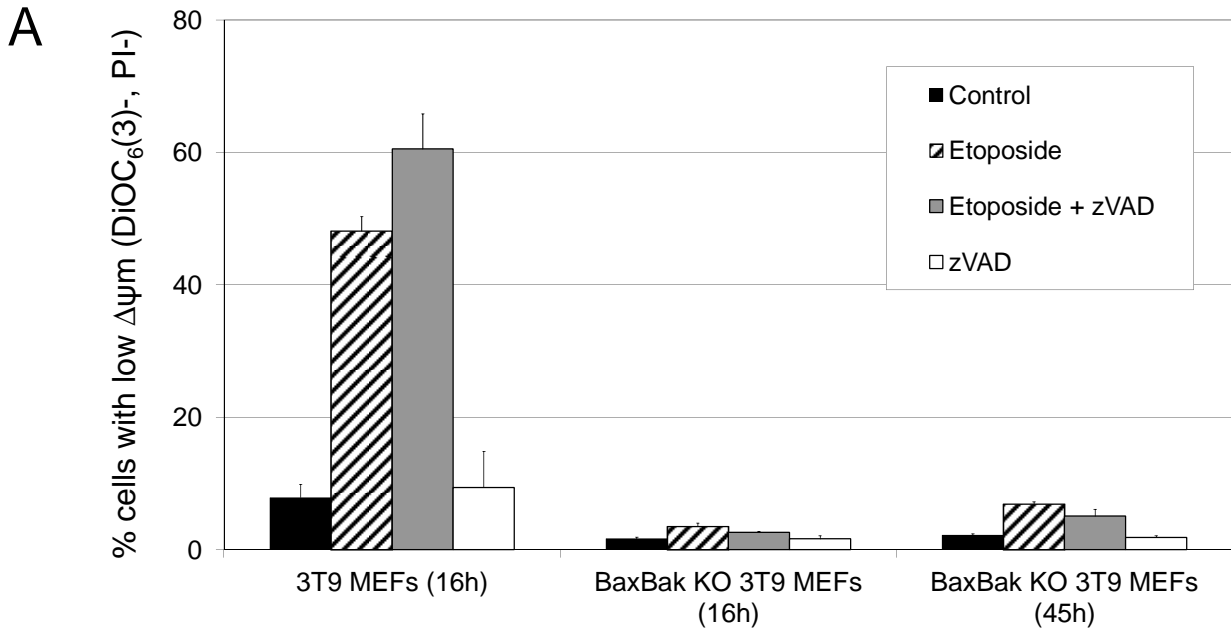


Figure 4

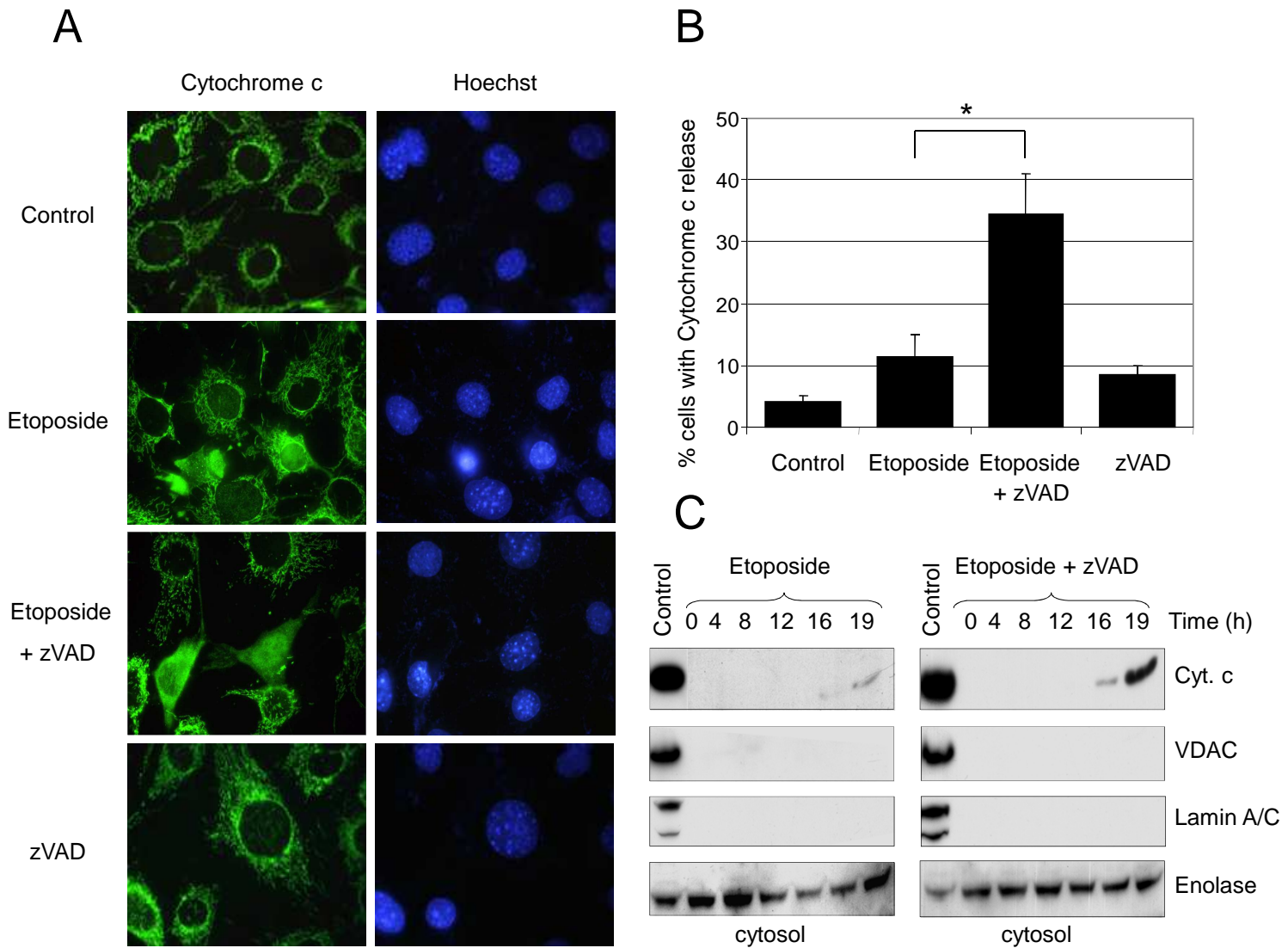


Figure 5

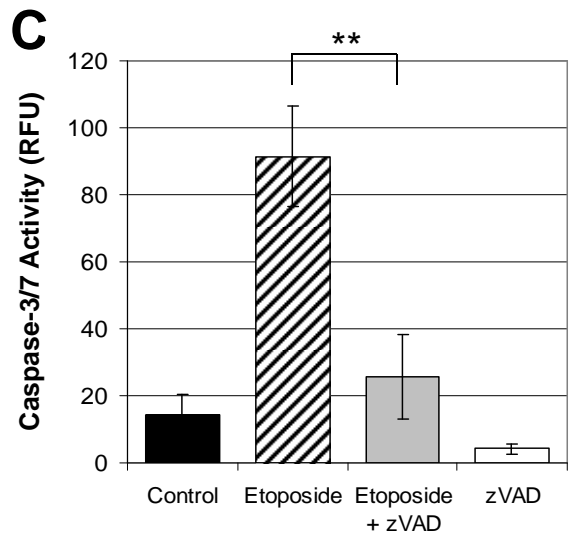
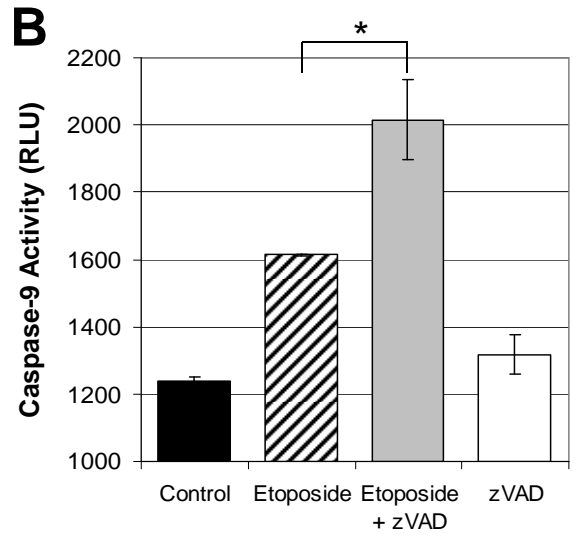
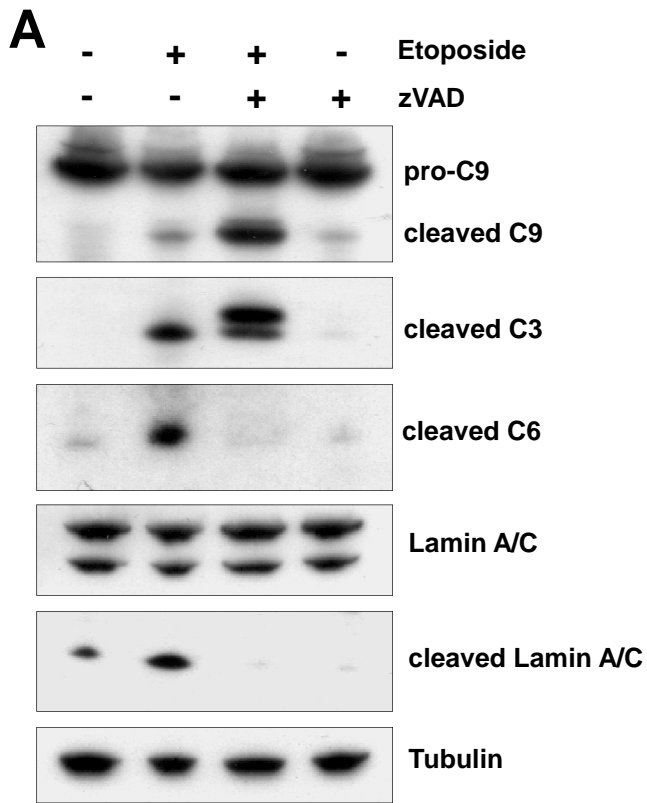


Figure 6

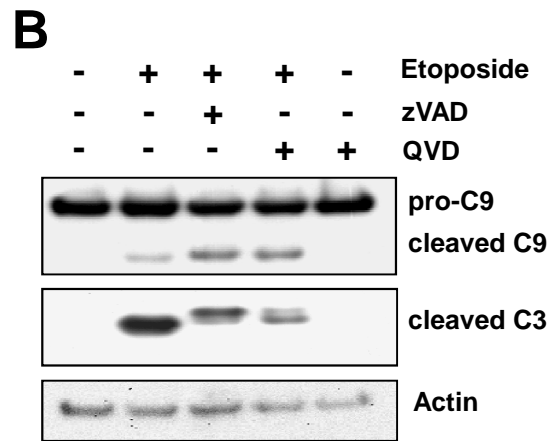
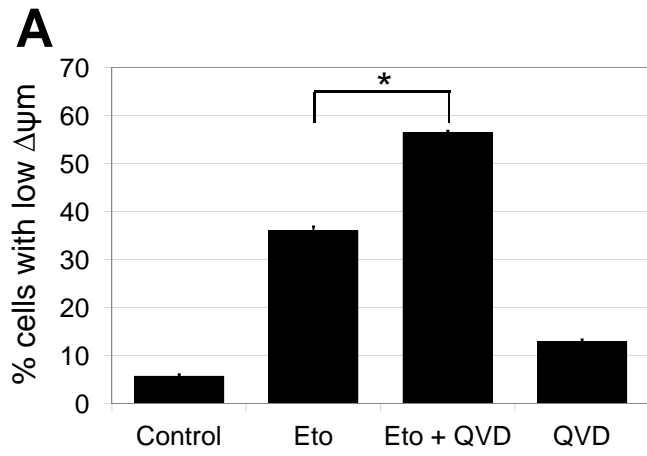


Figure 7

